The Expectation of the Energy Spectrum of Cosmic-Ray Electrons with LHAASO

Sha Wu[*]

Key Laboratory of Particle Astrophysics, Institute of High Energy Physics, Chinese Academy of Sciences, 100049 Beijing, P.R. China.
E-mail: wusha@ihep.ac.cn

Songzhan Chen

Key Laboratory of Particle Astrophysics, Institute of High Energy Physics, Chinese Academy of Sciences, 100049 Beijing, P.R. China.

Huihai He

Key Laboratory of Particle Astrophysics, Institute of High Energy Physics, Chinese Academy of Sciences, 100049 Beijing, P.R. China.

Sujie Lin

Key Laboratory of Particle Astrophysics, Institute of High Energy Physics, Chinese Academy of Sciences, 100049 Beijing, P.R. China.

Yuncheng Nan[†]

Institute of Frontier and Interdisciplinary Science and Key Laboratory of Particle Physics and Particle Irradiation (MOE), Shandong University, Qingdao, Shandong 266237, China .

On behalf of the LHAASO Collaboration

The high-energy electrons suffer severe energy loss during their propagation, owing to the Synchrotron and Inverse-Compton processes. Thus, the electrons exceeding TeV are most likely originating from few local sources, such as dark matter particle and astrophysical sources. The dipole anisotropy of the electrons is also regard as an unique signature about the nearby sources. With the merit of large detecting area and strong background suppression, the LHAASO experiment provides an opportunity on extending the detection of high-energy cosmic-ray electrons from 500 GeV to 100 TeV. In this paper, We explore the efficient rejection of hadronic background of LHAASO, in combination with KM2A and WCDA and make the expectation on the spectrum of cosmic-ray electrons and the sensitivity of dipole anisotropy with LHAASO. The influence on the research of electronic origin is also discussed.

36th International Cosmic Ray Conference -ICRC2019-
July 24th - August 1st, 2019
Madison, WI, U.S.A.

---

1. Introduction

Cosmic rays are high energy particles that come from outside of the solar system. They are mainly composed of protons, heliums and heavier nuclei, as well as a small fraction of electrons. In contrast to the hadronic cosmic rays, the lifetime and propagation distance of cosmic ray electrons (CREs) (in this paper, electrons always means the sum of electrons and positrons) is seriously limited by energy losses via synchrotron radiation and inverse Compton scattering. As discussed in [1], TeV electrons lost most of their energy on a time scale of 10^5 yr and their propagation distances are therefore confined by several hundred parsecs. Spatial distribution of nearby sources [1] and new cosmic ray propagation models [2] may produce significant deviations in the most energetic part of the observed spectrum compared to the conventional state calculated by the GALPROP interstellar propagation code [3]. Measuring the spectrum of CREs above TeV energy is important to constrain the models of the cosmic ray's propagation and search for the nearby sources. It provides a direct measurement about the local cosmic-ray accelerators and diffusion.

The CREs flux at 1 TeV (10TeV) is approximately 0.1% (0.01%) of the flux of hadronic particles. CREs are almost isotropic and always get mixed up with cosmic rays. We can't do background estimation like observing a gamma-ray source. Indirect measurement of CREs in ground experiments has always been a difficult problem due to the limitation of discrimination. With a large effective area and high background rejection, Large High Altitude Air Shower Observatory (LHAASO) may be able to directly measure cosmic-ray electron spectrum from several hundred GeV to one hundred TeV. And it provides a possibility for LHAASO to detect interesting features in the electron spectrum above TeV in the future.

This paper mainly makes the expectation on the energy spectrum and the dipole anisotropy of CREs with LHAASO. If the inconsistency of the strong interaction model can be controlled within 1%, LHAASO can measure the cosmic ray electron spectrum from 500GeV to 100TeV. When the systematic error of cosmic ray large-scale anisotropy is 0.01%, LHAASO can give a limit on the electron dipole anisotropy from 1TeV to 100TeV.

2. The LHAASO Detectors and Simulation

2.1 The LHAASO detector

LHAASO (Fig.1), built 4410 m a.s.l. near Daocheng, in the Sichuan province of China, mainly aims to very high energy gamma-ray astronomy and cosmic rays with energies in 10^{11}-10^{18} eV. In addition, LHAASO will play an important role in various aspects of physics researchs, including solar physics, large-scale cosmic ray anisotropy, Lorentz invariance violation and indirect DM search et al. Consisting of the following three major sub-arrays [4], LHAASO can measure different secondaries such as electrons, muons and Cherenkov/fluorescence photons.

- KM2A is made up of 5195 electromagnetic particle detectors (EDs) and 1171 muon detectors (MDs), covering an area of 1.3 km^2. 4901 EDs, each with an area of 1 m^2, are arranged on a triangular grid of 15 m spacing to cover a circular area with a radius of 575 m. The other 294 EDs, each with a space of 30 m, cover a circular area with radius from 575 m to 635 m in the surrounding region which can be used to decide if the core located inside the central area.

Each ED consists of 4 plastic scintillation tiles which is covered by a 0.5 cm thick lead plate to convert the gamma-rays to electron-positron pairs and improve the angular resolution of the array. The EDs detect mainly the electromagnetic particles in the shower to reconstruct the primary direction, core location, and energy. Each MD, a cylindrical water tank with diameter of 6.8 m and height of 1.2 m, is arranged on a triangular grid of 30 m spacing. The tank, buried under 2.5 m of soil is used to detect mainly the muonic component of showers to discriminate between gamma-ray/electrons and hadrons.

- WCDA, covering an area of about 78,000 m^2, is divided into 3 water ponds. With an effective water depth of 4 m, two of them cover an area of 150 m × 150 m, containing 900 detector units each. The other cover an area of 300 m × 110 m, containing 1320 detector units. Each detector unit is 5 m × 5 m and is divided by black plastic curtains. A 8-inch upward-facing photomultiplier tube (PMT) sits at the bottom center of each cell to collect Cherenkov light generated by shower secondary particles in water. In order to enlarge the dynamic range, a 1.5-inch PMT is placed aside each large PMT in one of the two smaller ponds.

- WFCTA consist of 12 wide-field-of-view Cherenkov telescopes. It is mainly used to detect Cherenkov/fluorescence photons produced in the air. In this work, we do not use this array.
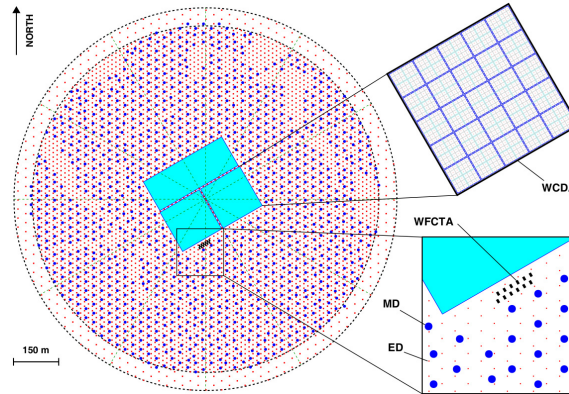

Figure 1: Layout of LHAASO detectors

2.2 LHAASO Detector Simulation

The EAS processes of electron and cosmic-ray hadrons both are carried out by CORSIKA [5] version 7.4005. QGSJETII-04 and GHEISHA are adopted as the hadronic interaction model for high energy and low energy respectively. For KM2A and WCDA detector response, a cell detector of KM2A and WCDA is simulated by GEANT4 program [6]. Then, the parameterized method presented in [7] was adopted here.

Electron showers are simulated with a power law spectrum with index of 2.59 from 100 GeV to 1 PeV. The zenith angles were sampled from 0° to 60°. The cores were sampled within a large enough circular area with a radius of 1000 m from the center of LHAASO. Below 1TeV, the electron spectrum is reweighted to measurement by AMS [8]. Above 1TeV, the electron spectrum is reweighted to measurement by HESS [9]. Additionally, cosmic-ray hadrons are simulated with

a power law spectrum index of 2.7 from 100 GeV to 1 PeV. The zenith angles and cores adopted the same sampling range as electrons. The cosmic-ray spectrum is reweighted to all particle flux derived by Gaisser et.al [10]. Another set of cosmic-ray hadrons were generated using the EPOS LHC package to test for consistency.

Random noises from a single secondary cosmic ray in the KM2A and WCDA are also taken into account. According to the KM2A engineering array result, the noise rate is approximately 2 kHz for each ED and the noise rate of each MD is about 6 kHz. According to the prototype array of approximately 1% scale of WCDA built at YangBaJing,Tibet,China, the noise rate of WCDA is averagely set to be 50 KHz

3. Electron-Hadron Separation

When an electromagnetic particle enters the atmosphere, it interacts with the nuclei in the air, resulting in an air shower that contains mostly lower energy electrons, positrons, and gamma-ray. On the other hand, hadronic cosmic-rays will undergo hadronic interactions with the nuclei in the air. This will give rise to charged pions that can decay into muons. These different properties can help LHAASO to separate the electron events from the hadron background.

3.1 Electron-Hadron Separation in WCDA

According to the lateral and longitudinal shower profiles of the secondary particles in the EAS induced by different primaries, four sensitive parameters are adopted by WCDA to separate gamma-rays from cosmic-rays background [11]. We use two of the most sensitive parameters to select electron showers. The first parameter, compactness, is defined as $C_{par} = nFit/cxPE_{45}$ where nFit is the number of fired PMTs during the reconstruction process and $cxPE_{45}$ is the effective charge measured in the PMT with the largest effective charge outside a radius of 45 m from the shower core. The second parameter, $P_{par} = \frac{\sum PE_{40}}{\sum PMT_{40}}$, which is the average density outside of 40 m from the shower core. In addition, detectors with photoelectron Numbers greater than 10 at a distance of 45 meters from the core are used to reconstruct the muon number M_{par}. The distribution of these three parameters is shown in Fig.2.

3.2 Electron-Hadron Separation in KM2A

Based on the fact that electron showers are muon-poor, the numbers of electromagnetic components N_e and muons N_μ can be used to discriminate original electron events from hadron background. The parameter R_{par} is defined as $R_{par} = N_\mu/N_e$. As a big Muon detector, locating at the center of LHAASO, WCDA can help KM2A do a better electron and hadron separation. We also use the parameter Pe_{max}, the maximum number of photoelectrons in the WCDA detector unit away from KM2A reconstruction core more than 40 m, and the parameter W_{mu}, the number of Muons that detected by WCDA, as the electron-hadron separation variable. The distribution of these three parameters is shown in Fig.3.

3.3 Separation Result

For electron and hadron discrimination, We use Boosted Decision Trees with a Gradient boosting algorithm (BDTG) as multi-variate analysis methods. BDTG can be easily implemented by
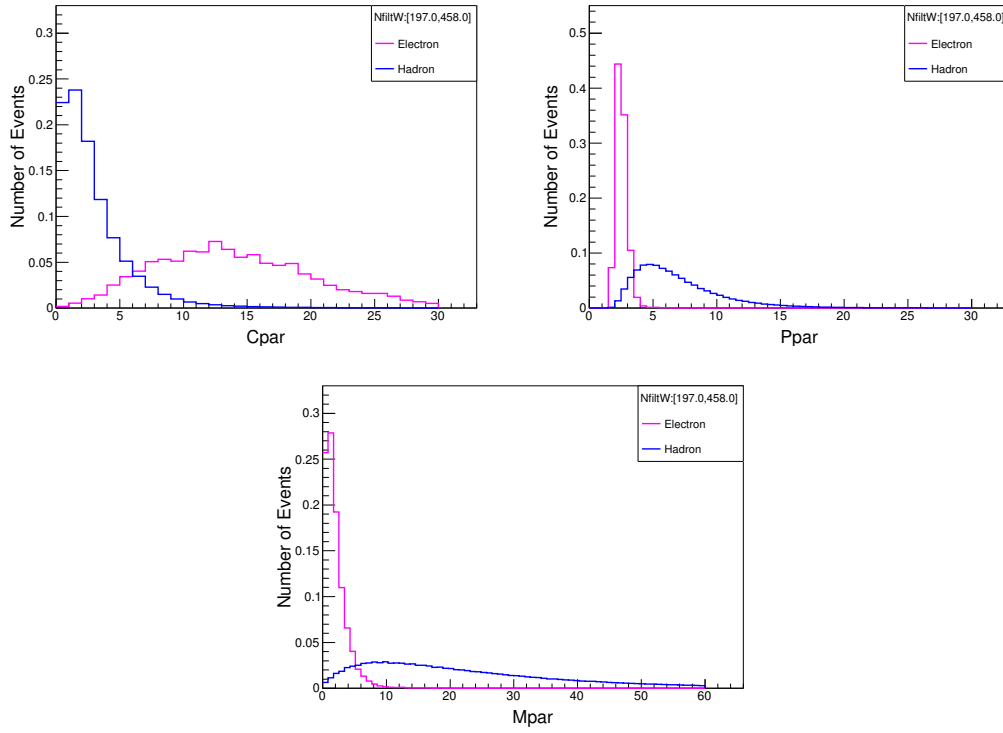
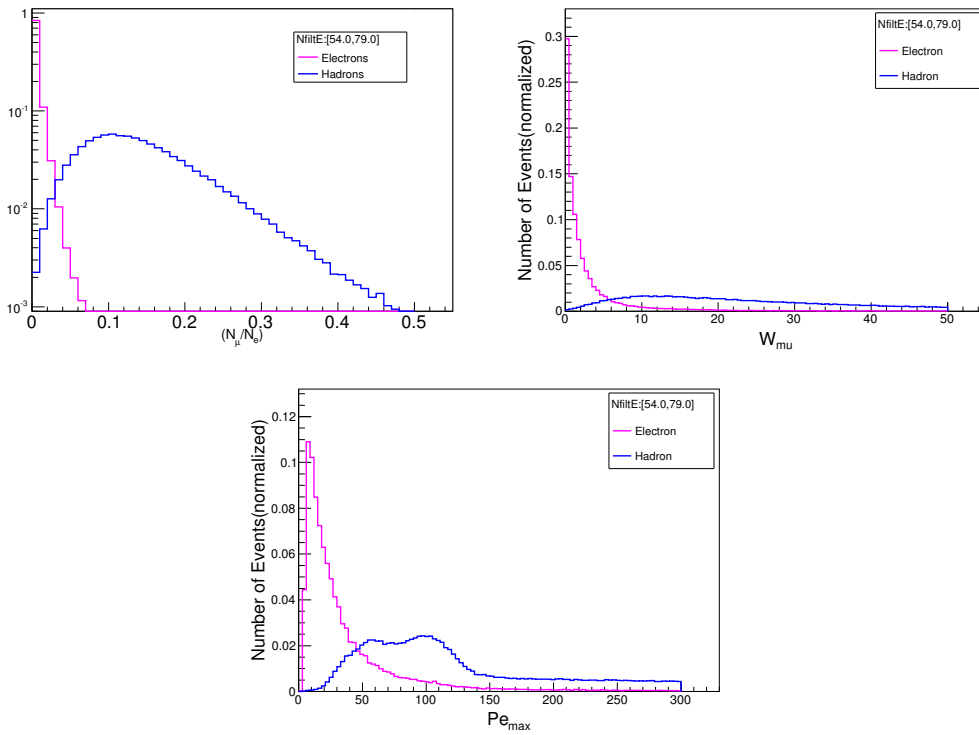**Figure 2:** Distribution of WCDA sensitivity parameters of electron and hadron Separation.

Figure 3: Distribution of KM2A sensitivity parameters of electron and hadron Separation.

using the ROOT TMVA [12] framework. It's almost certainly background when the return value is -1.0, and it is almost certainly an electron when return value is 1.0.

Fig.4 shows the predicted efficiency of electrons and hadronic background which pass the electron-hadron discrimination cuts. The efficiency of electrons is required to be greater than 30% while the hadronic background is preserved as little as possible. The rejection efficiency (the reciprocal of the remaining ratio) of hadrons is about 1×10^3 at 4 TeV and 1×10^5 at 100 TeV. Beyond about 100 TeV, none of the simulated background survive cuts which makes the analysis difficult to gain the best hadron rejection efficiency at high energy. Therefore, the last two points just show the upper limit of the hadron remaining efficiency.
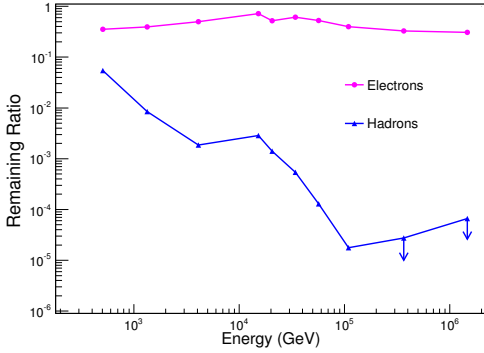
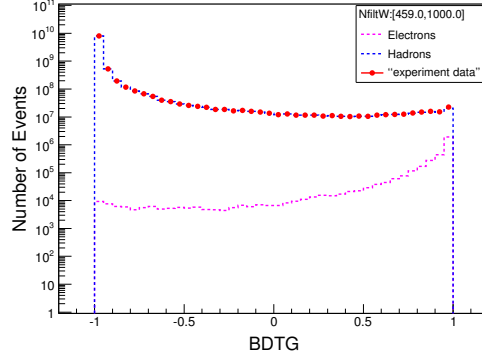**Figure 4:** The efficiency of electrons and hadronic background after discrimination cut is made

Figure 5: BDTG response of hadrons MC (blue dot line), electrons MC (pink line), and "experiment data"(red dot line)

4. Methods

Although there is good electrons and handrons separation, the remaining cosmic-ray background is comparable to the electrons. It is difficult to observe the isotropic CREs spectrum with LHAASO. Therefore, we try to get the most probable number of electrons in each energy band by fitting the BDTG response distribution.

Each simulated event is assigned a BDTG response value, from -1.0 to 1.0, where higher values indicate that the event is more signal-like. The distributions of BDTG response of MC electrons and hadrons can be well known from the simulation. Considering the statistical uncertainty, the "experiment data" distributions of BDTG response is sampled as poisson distribution. We select only those events with BDTG response values larger than 0.5, which contains the majority of the signal-like events and rejects the majority of the background-like events, showing in Fig.5. Then, we fitting the distributions of "experiment data" with the distributions of simulated electrons and hadrons in independent energy bands. The free parameter is the final electron fraction, $\varepsilon = \hat{N}_e / \hat{N}_t$, where $\hat{N}_e$ is the total number of "measured electrons" and $\hat{N}_t$ is the total number of "experiment data" in the remaining bins. The least squares equation is defined as:

$$\chi^2 = \sum \left(\frac{\hat{N}_{t,i} - [\varepsilon \hat{N}_t \frac{N_{e,i}}{\sum N_{e,i}} + (1-\varepsilon)\hat{N}_t \frac{N_{h,i}}{\sum N_{h,i}}]}{\sigma_i} \right)^2 \tag{4.1}$$

where $N_{h,i}$ is the number of MC hadrons in the remaining bins and $N_{e,i}$ is the number of MC electrons in the remaining bins. The number of "measured electrons" can be deduced as $\hat{N}_e = \varepsilon \times \hat{N}_t$ and the background $\hat{N}_h = (1-\varepsilon) \times \hat{N}_t$.

5. Result

5.1 Expect the Energy Spectrum of CREs

The expected CREs energy spectrum between 500GeV to 100TeV is shown in Fig.6. In actual measurement, the statistical errors of the simulated samples is not negligible and now it is dependent on the number of simulated events. It is clear that the existing statistics are very inadequate. The statistical error is estimated under the assumption that we have a tenth of a year's worth of simulated electrons and hadrons. In the future, we need dramatically enlarge our simulation sample for real data analysis. In fact, this will be a challenging job due to large time, computing and storage resource consuming. VERITAS [13] randomly chose 5.7 million events from the full data set to do the BDT train. This requires fewer CPU hours and is less dependent on the fidelity of the hadronic simulations.

Besides the statistical errors, some systematic errors will also affect the measurement of LHAASO on CREs, such as the uncertainties in energy estimation, the inherent hadronic interaction in the simulation, and so on. Assuming LHAASO has the same absolute energy scale with ARGO which is less than 13%. The influence on the CRE flux determination will be $\sim 42\%$. It is illustrated by shaded band in Fig.6.

To estimate the number of electron, the BDTG distributions obtained in simulation are used to fit the equation 4.1. The electron fraction is also tiny comparing to the proton background. Thus, this method will be strongly dependent on the reliability of the simulation, especially for proton simulation. To test the effect of the uncertainties in the proton simulation, a similar set of proton-initiated showers were generated using the EPOS LHC model. In general, the yielded BDTG distribution using the EPOS LHC model is consistent with that of QGSJETII-04 model, while, the distribution shows a slight rise toward BDTG response value equal to 1 and the rise is somewhat more pronounced for EPOS LHC as compared to QGSJETII-04 model. We artificially increase 1% to the gamma-ray like component to estimated systematic errors. The result is shown in Table.1. If the discrepancy is greater than 2%, the systematic errors is too large to observe the CREs.

5.2 Expect the Sensitivity to Dipole Anisotropy of CREs

We expect the sensitivity of CREs dipole anisotropy for one year of LHAASO simulation, showing in Fig.7. A small but measurable energy-dependent large-scale anisotropy (LSA) in the arrival direction distribution of galactic cosmic rays has been measured by different experiments in the past decades. According to recent results, the amplitude of the anisotropy is about 10^{-3} and the systematic error is about 10^{-4}. Considering a 10^{-4} systematic error of cosmic rays, we count the systematic error of CREs which is shown in Fig.7. LHAASO obviously can not see the anisotropy of G65.3+5.7 and the upper limits on the intrinsic DM anisotropy [15] in the first two Bins. However, it can give a strongest limit on CREs dipole anisotropy from 500GeV to 100TeV.
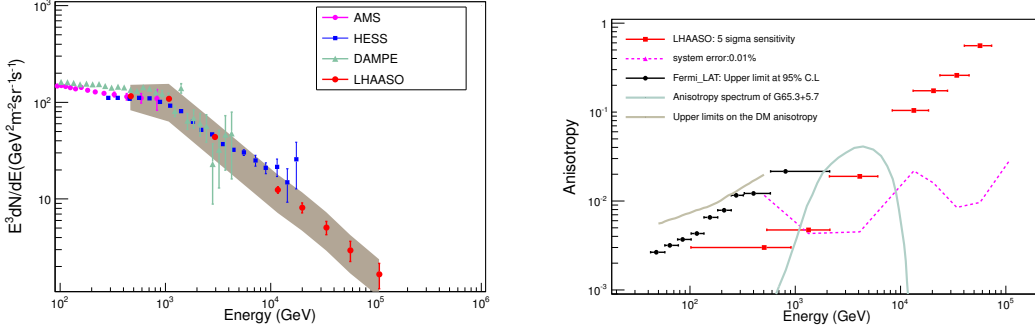
Figure 6: The expected on the energy spectrum of CREs comparing to measurements (as labeled [8],[9],[14]). The error bars are statistical. The shaded band indicates the approximate systematic error arising from uncertainties in the absolute energy scale.

Figure 7: The expectant sensitivity of CREs anisotropy. The black dots shows the upper limit at 95% C.L. on dipole anisotropy from Fermi. The pink dot line is the systematic error. The green line represents the anisotropy that contributed by local SNR G065.3+0.517 [16]. The grep line is the upper limits on the intrinsic DM anisotropy [15].

Bin	FCN	ε	ε_{error}	$\hat{N}_t$	$N_{e,MC}$	sys_{err}	$relative_{sys}$
1	80173	1.39×10^{-2}	8.61×10^{-6}	3.702×10^{10}	3.196×10^{8}	5.134×10^{8}	60.7%
2	4713	2.62×10^{-2}	2.49×10^{-5}	2.076×10^{9}	4.808×10^{7}	5.436×10^{7}	13.0%
3	168	2.50×10^{-2}	6.55×10^{-5}	1.415×10^{8}	3.155×10^{6}	3.539×10^{6}	12.2%
4	7.49	6.29×10^{-3}	1.99×10^{-4}	9.090×10^{6}	3.685×10^{4}	5.727×10^{4}	61.2%
5	4972	5.04×10^{-3}	1.96×10^{-4}	3.271×10^{9}	1.180×10^{7}	4.652×10^{6}	39.3%
6	702	8.15×10^{-3}	1.20×10^{-4}	1.099×10^{8}	5.498×10^{5}	3.472×10^{5}	63.1%
7	31	1.23×10^{-2}	2.61×10^{-4}	2.110×10^{7}	1.451×10^{5}	1.161×10^{5}	80.0%
8	5.83	1.78×10^{-2}	6.51×10^{-4}	2.697×10^{6}	3.403×10^{4}	1.312×10^{4}	37.4%
9	5.88	1.44×10^{-2}	8.55×10^{-4}	7.493×10^{5}	8.971×10^{3}	1.884×10^{3}	21.0%
10	4.76	4.28×10^{-3}	3.56×10^{-4}	5.886×10^{5}	2.358×10^{3}	1.651×10^{2}	6.9%

Table 1: The CREs Spectrum with systematic errors

6. Conclusions

The LHAASO is a new hybrid extensive air shower array which is already under construction. With very large area and strong electron-hadron discrimination capability, it is possible to perform a direct measurement for the CREs from 500 GeV to 100 TeV. Hence it may offer an efficient cross-validation on the spectral break of the electron around 1 TeV with high statistics, and explore the new structure beyond 10 TeV. Besides, the LHAASO also possesses strong sensitivity on the dipole anisotropy of the electrons, which is a unique tool in discrimination between the astrophysical origins and the DM origins.

HESS and VERITAS have adopt this kind of method to measure the CRE spectrum. However, it rely heavily on the BDTG distributions of the MC electrons and hadrons. With large duty cycle and effective area, the EAS array need much more simulated data to reduce the statistical errors. This is a great challenge of future work. The impact of model inconsistencies is significant. If the discrepancy is greater than 2%, we may can not see the CREs. This paper mainly introduce the

method of measuring the CREs and discuss the effects of statistical errors and systematic errors. Experimental data is needed to test whether we can observe CREs.

References

[1] K. Fang, et al. *Perspective on the Cosmic-ray Electron Spectrum above TeV*, *The Astrophysical Journal*, 836:172, February 2017.

[2] Z. Tian, et al. *Electron and positron spectra in the three dimensional spatial-dependent propagation model*, *arXiv:1904.10663v1*, April 2019.

[3] A. W. Strong and I. V. Moskalenko. *Models for galactic cosmic-ray propagation*, *Advances in Space Research*, 27:717-726, 2001.

[4] H. H. He. *Design of the LHAASO detectors*, *Radiation Detection Technology and Methods*, February 2018.

[5] D. Heck, J. Knapp, J. N. Capdevielle, G. Schatz, and T. Thouw. *CORSIKA: a Monte Carlo code to simulate extensive air showers*, February 1998.

[6] J. Allison, K. Amako, J. Apostolakis, et al. *Geant4 developments and applications*, *IEEE Transactions on Nuclear Science*, 53:270-278, February 2006.

[7] S. W. Cui, Y. Liu, and X. H. Ma. *Simulation on gamma ray astronomy research with LHAASO-KM2A*, *Astroparticle Physics*, 54:86-92, February 2014.

[8] M. Aguilar, D. Aisa, B. Alpat, et al. *Precision Measurement of the $(e^+ + e^-)$ Flux in Primary Cosmic Rays from 0.5 GeV to 1 TeV with the Alpha Magnetic Spectrometer on the International Space Station*, *Physical Review Letters*, 113(22):221102, November 2014.

[9] F. Aharonian, A. G. Akhperjanian, U. Barres de Almeida, et al. *Energy Spectrum of Cosmic-Ray Electrons at TeV Energies*, *Physical Review Letters*, 101(26):261104, December 2008.

[10] T. K. Gaisser. *Spectrum of cosmic-ray nucleons, kaon production, and the atmospheric muon charge ratio*, *Astroparticle Physics*, 35:801-806, July 2012.

[11] W. Y. Liao, et al. *Gamma/Proton separation study for the LHAASO-WCDA detector*, *ICRC 2017*.

[12] A. Hoecker, P. Speckmayer, J. Stelzer, et al. *TMVA-Toolkit for Multivariate Data Analysis.*, *ArXiv*,March 2007.

[13] A. Archer, W. Benbow, et al. *Measurement of cosmic-ray electrons at TeV energies by VERITAS PHYSICAL REVIEW D*, 98, 062004.

[14] DAMPE Collaboration, G. Ambrosi, Q. An, et al. *Direct detection of a break in the teraelectronvolt cosmic-ray spectrum of electrons and positrons*, *Nature*, 552:63-66, December 2017.

[15] E. Borriello, L. Maccione, and A. Cuoco. *Dark matter electron anisotropy: A universal upper limit.* *Astroparticle Physics*, 35:537-546, March 2012.

[16] K. Fang, X.J. Bi, and P.F. Yin. *Discriminating local sources of high-energy cosmic electrons and positrons by current and future anisotropy measurements. mnras*, 478:5660-5670, August 2018.